JOURNAL OF CATALYSIS 83, 19–24 (1983)

Kinetics of Carbidic Carbon Formation from CO in the 10^{-6}-Torr Range on Ni(110)

R. ROSEI,[1] F. CICCACCI, R. MEMEO, C. MARIANI,[2] L. S. CAPUTI, AND L. PAPAGNO

Dipartimento di Fisica dell'Università della Calabria, Arcavacata di Rende, Cosenza, Italy, and Gruppo Nazionale di Struttura della Materia

Received August 6, 1982; revised February 11, 1983

Kinetic measurements of the formation of carbidic carbon on a Ni(110) surface were taken by exposing the sample at different temperatures (200°C < T < 350°C) and different pressures (10^{-6} Torr < P_{CO} < 3×10^{-5} Torr). Carbidic carbon coverages on the surface were monitored by *in situ* Auger spectroscopy. Several different models for CO decomposition were considered and the relative rate equations compared with the experimental data. From this comparison we conclude that, in the pressure range of our work, CO on Ni(110) simply dissociates by the rupture of the CO bond. The activation energy of the process has been evaluated (23 kcal/mole) and found in excellent agreement with recent generalized valence bond calculations. Our finding, of course, does not imply that this is the dominant mechanism of carbon formation in Fischer–Tropsch synthesis (which is run at much higher CO pressures).

INTRODUCTION

A great amount of work has been done towards elucidating the mechanism of the methanation reaction and Fischer–Tropsch synthesis (FTS) (*1*) since the discovery that methane (*2*) and other hydrocarbons (*3*) can be synthesized from carbon monoxide and hydrogen. Scientific and commercial (*4*) interest in these reactions has recently been further stimulated by steep increases in prices and anticipated shortages in these fuels. Lately, besides the conventional experimental techniques of catalysis research, a new approach based on UHV techniques of surface science has been attempted (*5, 6*).

This approach has provided striking experimental evidence (*5–8*) that a surface form of "carbidic" carbon must be considered an important intermediate in the methanation reaction and FTS in general. This carbon species, which can also be produced by heating a transition metal catalyst in presence of CO (*5*), has a characteristic Auger lineshape, strongly reminiscent of carbon Auger spectra of transition metal carbides (from which fact it has been termed "carbidic" carbon (*5*)).

Carbon monoxide dissociation seems therefore a key step in the methanation reaction. Within this framework we have undertaken the present experimental work to address the following questions:

(i) Is it possible to monitor the kinetic of selected steps of the methanation reaction in the sub micro-Torr (1 Torr = 133.3 Nm^{-2}) pressure regime?

(ii) By which mechanism does the CO dissociate?

(iii) What are the rate constants and activation energies critical for the dissociation process?

In the following we report definite answers to the above questions, in the very low CO surface coverage regime. Further work (at much higher pressures) is needed, however, to elucidate the process of carbon formation in the FTS regime.

[1] Present address: Laboratorio di Fisica Atomica e Molecolare, Istituto di Fisica, Università di Trieste, Trieste, Italy.

[2] Present address: PULS, Laboratori Nazionali di Frascati, Frascati, Rome, Italy.

0021-9517/83 $3.00

EXPERIMENTAL

A Ni single crystal sample (4 × 7 × 1 mm^3) cut to expose the (110) face (within 1°) was polished with diamond paste to a mirror finish and chemically etched (60% acetic, 30% nitric, and 10% hydrocloric acid) to remove the damaged surface layer. The sample was mounted in a Varian UHV system routinely operated below 3×10^{-10} Torr and cleaned *in situ* with cycles of argon ion sputtering and annealing. The initial impurities (C, O, S) were easily removed by our cleaning procedure but sulfur kept slowly segregating from the bulk. The surface was judged "clean" when the level of sulfur was <0.003 ML.

After the cleaning procedure the sample was heated to the operating temperature 200°C ≤ T ≤ 350°C and high purity CO was admitted to the chamber from a reservoir through a leak valve up to the operating pressure, typically $10^{-7} \leq p_{CO} \leq 10^{-5}$ Torr. The ion pumps were throttled during these exposure periods while keeping a continuous leak from the reservoir to keep the CO partial pressure constant and the gas clean.

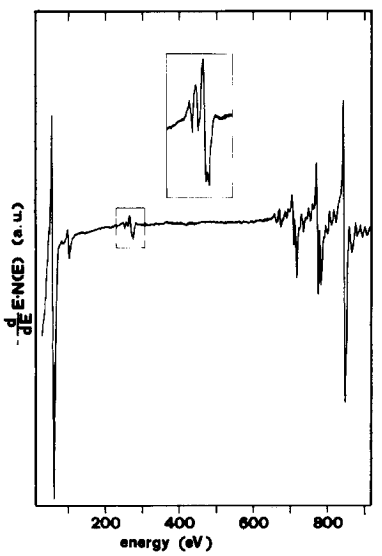

FIG. 1. Auger spectrum of a Ni(110) surface after 40 min exposure to CO at 6×10^{-6} Torr and T = 550 K. Only the Ni and C peaks are present. The insert shows that the carbon signal has the characteristic lineshape of "carbidic" carbon (*5*).

After an exposure period of several minutes the leak valve was closed and the CO pumped away. After a few minutes the chamber was back in the low 10^{-10} Torr range and an Auger spectrum of the surface was taken. During these operations the temperature of the sample was kept constant and always well above the desorption temperature of CO (~450 K). From the isosteres measurements in the literature (*9*) we estimate the coverage of CO during exposures as 0.003 ML ≤ ϑ_{CO} ≤ 0.04 ML (depending on the operating pressure p_{CO} and sample temperature) while during the Auger measurement $\vartheta_{CO} < 10^{-6}$ ML.

The procedure was then repeated for a new period of exposure at the same operating CO pressure and sample temperature, and the accumulation of carbon on the surface was measured again with Auger spectroscopy.

Figure 1 shows the Auger spectrum of the Ni(110) surface after a total exposure of 40 min at 6×10^{-6} Torr and T = 550 K. It is easily seen that the spectrum exhibits only the Ni and carbon peaks and that *no other impurity*[3] (at measurable level) is present. Note in particular that no oxygen is present. The inset in Fig. 1 shows an enlargement of the carbon Auger spectrum which has the well-known "carbidic" lineshape. Figure 2 shows the kinetics of carbidic carbon formation[4] on the Ni(110) surface at T = 550 K and $p_{CO} = 6 \times 10^{-6}$ Torr. Several different runs were completed with CO partial pressure ranging from 10^{-6} to 3×10^{-5} Torr and different sample temperatures (200°C ≤ T ≤ 350°C).

[3] Of particular significance is the complete absence of Fe impurities (which in principle could accumulate on the sample via dissociation of Fe carbonyls). Even small traces of Fe could considerably alter the CO dissociation rates.

[4] The carbon coverages were derived from the peak-to-peak height ratios of C and Ni_{848} Auger lines, weighted by the relative sensitivity factors. The different escape depths of the Ni and C Auger electrons were taken into account, assuming the carbon to be uniformly located on the surface layer.

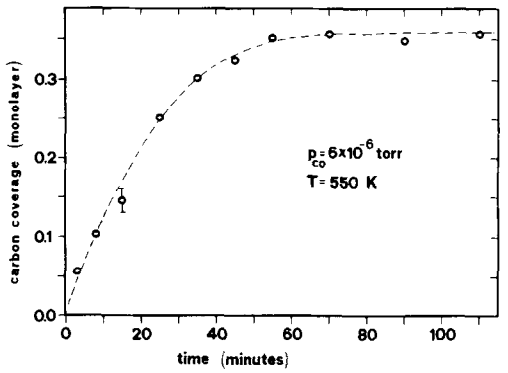

FIG. 2. Kinetics of "carbidic" carbon formation on a Ni(110) surface, $T = 550$ K and $p_{CO} = 6 \times 10^{-6}$ Torr. The circles represent the experimental points. The dashed line is intended as a guide for the eye.

KINETIC MODELS

In absence of hydrogen, one can consider three possible models for CO reaction with a transition metal which lead to the accumulation of carbon on the surface.

Figure 3 shows schematically the mechanisms involved in each model. Kinetics and rate equations for each model are discussed in the Appendix. The first step is, in any case, the adsorption of the CO molecule on the surface. In Model 1, this step is followed by direct dissociation into adsorbed carbon and oxygen. The third step involves the reduction of surface oxygen with CO and production of CO_2, which desorbs. In the second model two adsorbed CO molecules react forming CO_2 and leaving a carbon atom on the surface. Finally, in the third model an adsorbed CO molecule reacts with CO in the gas phase again producing CO_2 and surface carbon. In principle all three models can work, although disproportionation of CO ($2CO \rightarrow C_{(ads)} + CO_{2(gas)}$) is thermodynamically favored (*10*). It seems very important to be able to distinguish by which model the reaction takes place to guide future theoretical calculations.

Accordingly we have set up computer programs for comparing our kinetic data to the results of the mathematical rate equations predicted by each model. It was found that only Model 1 leads to good fits of different sets of experimental data taken at different pressures.

The results of such a fit are shown in Fig. 4. It should be noted that the coefficients K_1

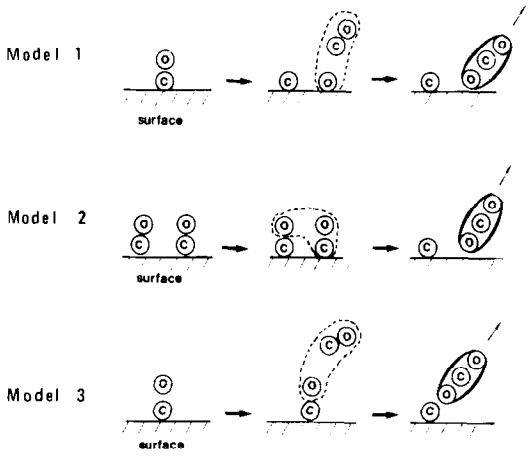

FIG. 3. Schematic description of possible CO dissociation models.

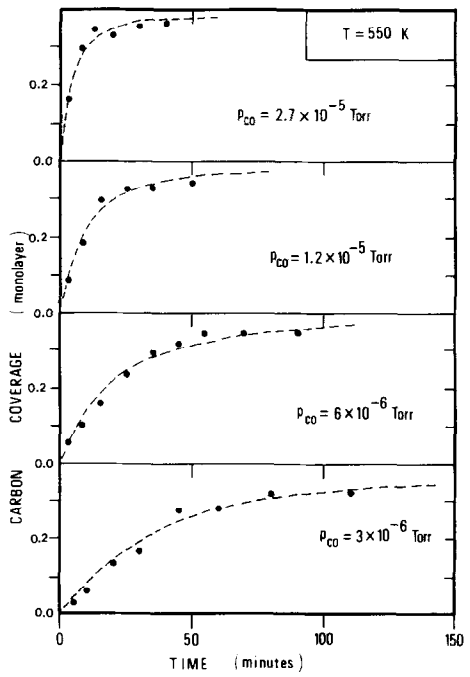

FIG. 4. Kinetics of carbidic carbon formation at $T =$ 550 K and different CO pressures. The dashed line through the experimental points represents the best fit obtained through Model 1 (see Appendix) and $K_2 = 4 \times 10^{-2}$ (monolayer $\times$ sec)$^{-1}$.

and K_{-1} were obtained from the literature (for the definition of the K coefficients see the Appendix). For K_3 only a lower limit can be obtained from the fit (because in no case was oxygen detected on the surface). It follows that the *only adjustable parameter* for fitting the entire set of data (at a given temperature) is K_2.

The fit we obtain is very good. The other two models never provided comparably good fits for the entire set of data. Usually, even though we could find K_2 values that would fit the curve at lowest pressure, the fit obtained for the higher pressures by using the equations of Model 2 and Model 3 was very poor. This finding is shown in Fig. 5. This figure reports "experimental" approximate rates obtained by assuming a Langmuir behavior for the carbon deposition. We have forced our models in such a way that they would give a good fit for $p_{CO} = 3 \times 10^{-6}$ Torr and determined a K_2 value for each model. We see that the behavior predicted by Model 1 is very close to the experimental findings while the rates predicted by Models 2 and 3 diverge at the higher pressures.

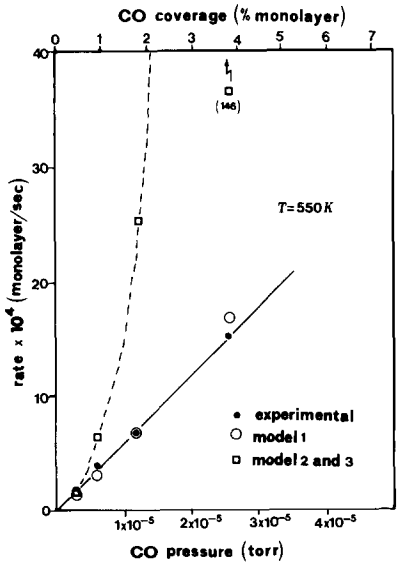

FIG. 5. Rate of carbidic carbon formation vs CO pressure at $T = 550$ K. The coefficient K_2 was chosen in such a way that each model would fit the lowest pressure experimental point.

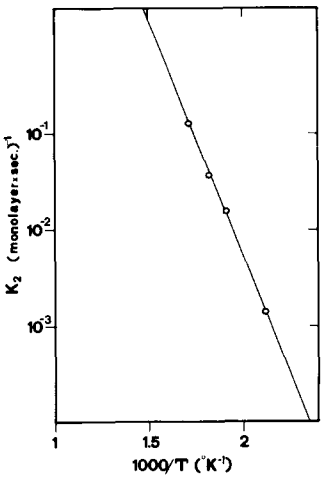

FIG. 6. Plot of log K_2 vs $10^3/T$. From the slope of this plot the activation energy for CO dissociation E_a ($K_2 = K_2^0 \exp(-E_a/RT)$) is obtained: $E_a = 23$ Kcal/mole.

Our results eliminate Models 2 and 3 as mechanisms for carbide formation, and are reasonably explained by Model 1.

We have taken complete kinetic data also at several other temperatures and in each case we have evaluated the rate constant that is proportional to K_2. Figure 6 is a plot of log K_2 vs the inverse absolute temperature; the activation energy for CO dissociation obtained from the slope of this plot is 23 kcal/mole. To our knowledge this is the first experimental determination of the activation energy for CO dissociation. Theoretical evaluation by Miyazaki (*11*) and Upton (*12*) give 23.4 and 23 kcal/mole, respectively, in exceedingly good agreement with our results.

In conclusion, in the present work we have shown that the kinetics of dissociation of CO on a Ni(110) single crystal can be followed directly via Auger spectroscopy by monitoring the carbidic carbon accumulation in the p_{CO} pressure range 10^{-6}–10^{-5} Torr. We have also shown that the experimental data provide strong evidence that the CO disproportionation in this pressure range proceeds via the rupture of the CO

bond and subsequent reduction of the surface oxygen. Finally, our data provide the first experimental determination of the activation energy for the dissociation of CO molecules adsorbed on a transition metal.

APPENDIX

Referring to Fig. 3, it is possible to consider, for the three models, the following reactions and the corresponding equations:

Model 1

$$\left.\begin{aligned} &CO_{(gas)} + * \underset{K_{-1}}{\overset{K_1}{\rightleftarrows}} CO^*_{(ads)} \\ &CO^*_{(ads)} + * \xrightarrow[K_2]{} C^*_{(ads)} + O^*_{(ads)} \\ &O^*_{(ads)} + CO_{(gas)} \xrightarrow{K_3} * + CO_{2(gas)} \end{aligned}\right\} \begin{cases} \dfrac{d\vartheta_{CO}}{dt} = K_1 p_{CO}\vartheta_v - K_{-1}\vartheta_{CO} - \dfrac{d\vartheta_C}{dt} \\ \dfrac{d\vartheta_C}{dt} = K_2\vartheta_{CO}\vartheta_v \\ \dfrac{d\vartheta_O}{dt} = K_2\vartheta_{CO}\vartheta_v - K_3 p_{CO}\vartheta_O \end{cases}$$

Model 2

$$\left.\begin{aligned} &CO_{(gas)} + * \rightleftarrows CO^*_{(ads)} \\ &CO^*_{(ads)} + CO^*_{(ads)} \xrightarrow{K_2} * + C^*_{(ads)} + CO_{2(gas)} \end{aligned}\right\} \begin{cases} \dfrac{d\vartheta_{CO}}{dt} = K_1 p_{CO}\vartheta_v - K_{-1}\vartheta_{CO} - \dfrac{d\vartheta_C}{dt} \\ \dfrac{d\vartheta_C}{dt} = K_2\vartheta_{CO}^2 \end{cases}$$

Model 3

$$\left.\begin{aligned} &CO^*_{(gas)} + * \rightleftarrows CO^*_{(ads)} \\ &CO^*_{(ads)} + CO_{(gas)} \xrightarrow[K_2]{} C^*_{(ads)} + CO_{2(gas)} \end{aligned}\right\} \begin{cases} \dfrac{d\vartheta_{CO}}{dt} = K_1 p_{CO}\vartheta_v - K_{-1}\vartheta_{CO} - \dfrac{d\vartheta_C}{dt} \\ \dfrac{d\vartheta_C}{dt} = K_2 p_{CO}\vartheta_{CO} \end{cases}$$

where ϑ_{CO}, ϑ_C, and ϑ_O are the coverages (in monolayer) of carbon monoxide, carbidic carbon, and oxygen; ϑ_v is the fraction of the surface Ni atoms left free from adsorbed species. K_1 and K_{-1}, related to the adsorption and desorption of CO on Ni, have been taken from the literature (*9*). K_2 is proportional to the rate of formation of carbidic carbon and has been found by fitting the experimental data with the numerical solution of the above equations; the coefficient K_3 takes account of the removal of oxygen from the surface in Model 1. Note that Models 2 and 3 can be seen as a single one, since the corresponding equations are identical, as can be seen considering that in our pressure range ϑ_{CO} is proportional to p_{CO} (cf. also Fig. 5).

ACKNOWLEDGMENTS

The authors acknowledge very useful discussion with Dr. D. W. Goodman, Dr. J. M. White, and Professor R. H. Hansen. A critical reading of the manuscript by Professor Hansen is also much appreciated.

REFERENCES

1. Bell, A. T., *Catal. Rev. Sci. Eng.* **23,** 203 (1981) and references therein; Lectures of the International Summer School on Surface Science and Catalysis of the Methanation Reaction, Sangineto Lido, July 1–10, 1982, unpublished.
2. Sabatier, P., and Senderens, J. B., *C.R. Acad. Sci.* **134,** 514 (1902).
3. Fischer, F., and Tropsch, H., *Chem. Ber.* **59,** 830 (1926).
4. Haggin, J., *Chem. Eng. News* **59,** 22 (1981).
5. Goodman, D. W., Kelley, R D., Madey, T. E., and Yates, J. T., Jr., *J. Catal.* **63,** 226 (1980).

6. Bonzel, H. P., and Krebs, H. J., *Surf. Sci.* **91,** 499 (1980).
7. Goodman, D. W., Kelley, R. D., Madey, T. E., and White, J. M., *J. Vac. Sci. Technol.* **17,** 143 (1980).
8. Goodman, D. W., Kelley, R. D., Madey, T. E., and White, J. M., *J. Catal.* **64,** 479 (1980).
9. Madden, H. H., Küppers, J., and Ertl, G., *J. Chem. Phys.* **58,** 3401 (1973).
10. Keim, E. G., Labohm, F., Gijzeman, O. L. J., Bootsma, G. A., and Geus, J. W., *Surf. Sci.* **112,** 52 (1981).
11. Miyazaki, E., *J. Catal.* **65,** 84 (1980).
12. Upton, T. H., Lectures of the International Summer School on Surface Science and Catalysis of the Methanation Reaction, Sangineto Lido, July 1–10, 1982, unpublished.